Hue Processing in Tetrachromatic Spaces

Alfredo Restrepo (Palacios)

Laboratorio de Señales; http://labsenales.uniandes.edu.co
Departamento de Ing. Electrica y Electronica, Universidad de los Andes,
Carrera 1 No. 18A - 70; of. ML-427, Bogota, Colombia;

ABSTRACT

We derive colour spaces of the hue-colourfulness-luminance type, on the basis of a four-dimensional hypercube. We derive a chromatic 2D hue that goes together with chromatic saturation and luminance, a toroidal hue that goes together with a toroidal saturation and colourfulness, and also, a 3D tint that goes together with colourfulness.

Keywords: Tetrachromacy, colour space, hypercube, double cone, Runge.

1. INTRODUCTION

A tetrachromatic image of $N \times M$ pixels can be modeled as a function $i : N \times M \to [0,1]^4$ where the interval $[0,1]$ represents the set of possible values in each of four, possibly overlapping, spectral bands. The total gammut of the possible colours a pixel can take is therefore the hypercube $[0,1]^4$. In the hypercube we identify the *black (or "schwartz") vertex* $\mathbf{s} := [0000]$, and the *white vertex* $\mathbf{w} := [1111]$; also, the subset $\mathbf{A} := \{(t,t,t,t) : t \in [0,1]\}$, the *achromatic segment* between $\mathbf{s}$ and $\mathbf{w}$. Tetrachromatic images can be visualized by feeding the RGB channels of a projector or screen with 3 of the bands, in one or several of the of the $3!\binom{4}{3} = 24$ possible ways of doing this. Several closed surfaces and a closed 3-manifold are identified in the hypercube, they are used to define hue for tetrachromatic colours. The modification of hue in tetrachromatic spaces can be used to attain interesting effects in the corresponding images, and also, in tetrachromatic artificial vision. See also,[1,2] and cite.

In addition to rods, which are effectively knocked out by excessive irradiance during the day, most mammals have only two types of cone receptors, dolphins have only one and frugivorous primates, as we are, have three. Many fish, birds and reptiles have 4, or more, cone receptor types. In the Bayer mosaic of a digital camera, the RGB filters provide three bands at disjoint pixels that are susequenly *interpolated*[3] at each pixel location, so that the number of pixels in the resulting image is the same as that in the Bayer pattern. In photographic cameras,[4,5] as part of the developing field of computatinal photography, in addition to the R, G and B filtered pixels, there are NIR, UV or *panchromatic pixels*[6] that are exposed to unfiltered light (in the spectrum band where the lens transmits the light and where the photoelectric transduction occurs) that include a significant amount of energy in the NIR (near infrared) band. If the response of the RGB pixels is subtracted from the response of a panchromatic pixel, a band of NIR+UVA results, where the energy of the two ends of the spectrum is mixed. Süsttrunk has taken advantage of the fact that NIR light, having a longer wavelength than visible light, effectively smooths out minute details in the scene being photographed; on the other hand, the use of UV light, instead of IR, together with the appropriate optics, can be exploited for imaginery where detail is important, e.g. in scientific imaginery. In multispectral imaging, bands of 20 nm cover the visible spectrum and sometimes IR and UV as well. We integrate the responses in 4 bands to test our methods.

2. GEOMETRY AND 4D COLOUR

The *set* of 81 *elements* given by the 16 vertices, the 32 edges, the 24 square faces and the 8 solid cubes of the hypercube boundary (8-24+32-16=0: the Euler characteristic of every closed 3-manifold is zero[7] and the boundary of the hypercube is a topological 3-sphere) together with the tetradimensional hypercube itself, is the 4-D *linear cell complex* K.

Email: arestrep@uniandes.edu.co; Telephone: (+57) 1 339 4949 ×2827

The subset of K given by the elements of dimension 3 or less, a 3-cell complex, is the *3-skeleton* of K; the union of its elements is the boundary $\mathbf{T} := \partial\mathbf{I}^4$ of the hypercube $\mathbf{I}^4 \subset \mathbf{R}^4$. A colour $[w, x, y, z] \in [0, 1]^4$ is on $\mathbf{T}$ if at least one of its coordinates is 0 or 1; indeed, we write $\mathbf{T} = \{w = 0\} \cup \{w = 1\} \cup \{x = 0\} \cup \{x = 1\} \cup \{y = 0\} \cup \{y = 1\} \cup \{z = 0\} \cup \{z = 1\}$. $\mathbf{T}$ is a *piecewise linear* (PL) tridimensional sphere that can be homeomorphed to a more standard, *round* $\mathbf{S}^3$.

The subset of K given by the elements of dimension 2 or less is the 2-skeleton K_2 of K; the union $|K_2|$ of its elements is not a manifold due to the presence of line segments from which more than 2 (in fact 3) square faces emerge; similarly, $|K_1|$ is not a 1-manifold since from each vertex, 4 edges emerge. In $|K_2|$ you find 8 PL 2-spheres, of 24 faces each, and 3 PL Heegaard tori of 16 faces each. These manifolds can be used geometrically to define *orientations* of the points in the hypercube that, with corresponding coordinate systems, is used to define several types of *hue* for 4D colours.

2.1 Tint

Tint is a "3D hue;" black and white are tints. Denote the central point of the hypercube as $\mathbf{g} = [\frac{1}{2}, \frac{1}{2}, \frac{1}{2}, \frac{1}{2}]$. To give *"spherical" coordinates* (d, Θ) to any point $\mathbf{p} \in \mathbf{I}^4$, let d be a measure of the distance between $\mathbf{p}$ and $\mathbf{g}$ (for example, the *max* of the absolute values of the components of $\mathbf{p} - \mathbf{g}^*$), and let $\Theta \in \mathbf{T}$ be the point where the ray from $\mathbf{g}$ through $\mathbf{p}$ leaves the hypercube. Call Θ the *tint*, or *generalized hue*, and call d the *colourfulness*, or *generalized saturation* of $\mathbf{p}$. In this sense, $\mathbf{T}$ is the set of tints. Note that $\mathbf{s}$ (black) and $\mathbf{w}$ (white) are fully colourful and are tints.

2.2 Chromatic Hue

Chromatic hue is two-dimensional; points in $\mathbf{A}$, including $\mathbf{s}$ and $\mathbf{w}$, are said to be achromatic and have no defined (chromatic) hue. Consider the $\binom{4}{2}2 = 12$ faces that do not meet neither the vertex $\mathbf{s}$ nor the vertex $\mathbf{w}$. You get a polyhedron, an "equatorial," topological 2-sphere, "linked" with the achromatic line, that we use to define a *chromatic hue* (i.e. a hue that is undefined for points on $\mathbf{A}$). Call this polyhedron the *chromatic dodecahedron,* given by $\mathbf{D} := \{w = 0, x = 1\} \cup \{w = 1, x = 0\} \cup \{w = 0, y = 1\} \cup \{w = 1, y = 0\} \cup \{w = 0, z = 1\} \cup \{w = 1, z = 0\} \cup \{x = 0, y = 1\} \cup \{x = 1, y = 0\} \cup \{x = 0, z = 1\} \cup \{x = 1, z = 0\} \cup \{y = 0, z = 1\} \cup \{y = 1, z = 0\}$. Each of the faces of $\mathbf{D}$ has a "primary" w, x, y or z at its fullest value 1, and another at its minimum value 0. Each square face of $\mathbf{D}$ is further subdivided into two triangles so that the points in each triangle obey the same ordering of their coordinates; e.g. the triangle with vertices $[0, 1, 0, 1]$ $[0, 1, 0, 0]$ $[1, 1, 0, 1]$ of points $[w, x, y, z]$ with $y \leq w \leq z \leq x$, and the triangle $[1, 1, 0, 0]$ $[0, 1, 0, 0]$ $[1, 1, 0, 1]$ of points $[w, x, y, z]$ with $y \leq z \leq w \leq x$, are the subdivision of the face $\{x = 1, y = 0\}$ of points $[w, x, y, z]$ with $min\{w, x, y, z\} = y$ and $max\{w, x, y, z\} = x$. There are 24 such *ordering triangles*; together, they give the subdivision of $\mathbf{D}$ called the *chromatic icositetrahedron* $\mathbf{IT}$. $\mathbf{IT} = \mathbf{D}$ is the set of (chromatic) hues; on each ordering triangle $\Delta \subset \mathbf{IT}$, the relative contribution of the *primaries* is fixed; each ordering representing a *hue family.*

To get the hue family corresponding to a chromatic colour (not in $\mathbf{A}$,) you may find out the permutation that orders its coordinates. More precisely, the hue $\mathbf{h}$ of $\mathbf{p} := [w, x, y, z]$ is the point $\mathbf{h} \in \Delta_h \subset \mathbf{IT}$ that is obtained as $\mathbf{h} = \frac{1}{\rho}[w, x, y, z] - \frac{\nu}{\rho}[1, 1, 1, 1]$ where ρ is the *chromatic saturation* given by the range of the primaries, and ν is the min. Note that at least one coordinate of $\mathbf{h}$ has value 1 and another, 0. Each chromatic point $\mathbf{p}$ is in the unique *chromatic triangle* $\Lambda_h = \mathbf{w\_s\_h}$; $\Delta_h \cup \Lambda_h = \mathbf{h}$. Indeed $[wxyz] = (1-\zeta)\mathbf{s} + \rho\mathbf{h} + \nu[1111]$, where ζ is the max of the primaries, is an expresion with barycentric coordinates $[1-\zeta, \nu, \rho]$, in the plane spanned by the points $\mathbf{s}$, $\mathbf{w}$ and $\mathbf{h}$.

2.3 Hue in a rhombic dodecahedron

When the points of $\mathbf{R}^4$ are projected along the direction [1111] onto the 3-subspace (through the origin)[†], $\mathbf{D}$ projects, without self-intersections, to a 2D rhombic dodecahedron[‡]. The achromatic segment projects to the

[*] The set of points $[x_0, x_1, x_2, x_3]$ with $\max\{x_i\} = r$ is the boundary of the hypercube of side $2r$, centered at the origin.

[†] This is computed by subtracting the average of the primaries from each primary.

[‡] The rhombic dodecahedron is a Catalan solid, i.e. a polyhedron that is dual to an Archimedean solid; in this case, to the cuboctahedron, which has 12 vertices, 24 edges, 8 triangle faces and 6 square faces; two triangles and two squares meet at each vertex.

central point of the enclosed solid rhombic dodecahedron and the cubes in $\mathbf{T}$ project to overlapping parallelepipeds in it. The points $\mathbf{a} = [\sqrt{\frac{3}{4}}, -\sqrt{\frac{1}{12}}, -\sqrt{\frac{1}{12}}, -\sqrt{\frac{1}{12}}]$, $\mathbf{b} = [0, \sqrt{\frac{2}{3}}, -\sqrt{\frac{1}{6}}, -\sqrt{\frac{1}{6}}]$ and $\mathbf{c} = [0, 0, \sqrt{\frac{1}{2}}, -\sqrt{\frac{1}{2}}]$ form an orthonormal basis that gives 3D coordinates to the projection space. The coordinates of the projections of the vertices of $\mathbf{D}$ are shown in Table 1.

Table 1. The 14 vertices of the chromatic dodecahedron are projected onto the 3-subspace normal to [1,1,1,1]. Then, the projections are given 3-space coordinates in the third column, which provide an embedding in 3-space of $\mathbf{D}$.

vertex	projection	[a, b, c]
0111	$[-\frac{3}{4}, \frac{1}{4}, \frac{1}{4}, \frac{1}{4}]$	[-0.8660, 0, 0]
0010	$[-\frac{1}{4}, -\frac{1}{4}, \frac{3}{4}, -\frac{1}{4}]$	[-0.2887, -0.4082, 0.7071]
0011	$[-\frac{1}{2}, -\frac{1}{2}, \frac{1}{2}, \frac{1}{2}]$	[-0.5774, -0.8165, 0]
0001	$[-\frac{1}{4}, -\frac{1}{4}, -\frac{1}{4}, \frac{3}{4}]$	[-0.2887, -0.4082, -0.7071]
0101	$[-\frac{1}{2}, \frac{1}{2}, -\frac{1}{2}, \frac{1}{2}]$	[-0.5774, 0.4082, -0.7071]
0100	$[-\frac{1}{4}, \frac{3}{4}, -\frac{1}{4}, -\frac{1}{4}]$	[-0.2887, 0.8165, 0]
0110	$[-\frac{1}{2}, \frac{1}{2}, \frac{1}{2}, -\frac{1}{2}]$	[-0.5774, 0.4082, 0.7071]
1010	$[\frac{1}{2}, -\frac{1}{2}, \frac{1}{2}, -\frac{1}{2}]$	[0.5774, -0.4082, 0.7071]
1011	$[\frac{1}{4}, -\frac{3}{4}, \frac{1}{4}, \frac{1}{4}]$	[-0.2887, -0.8165, 0]
1001	$[\frac{1}{2}, -\frac{1}{2}, -\frac{1}{2}, \frac{1}{2}]$	[0.5774, -0.4082, -0.7071]
1101	$[\frac{1}{4}, \frac{1}{4}, -\frac{3}{4}, \frac{1}{4}]$	[0.2887, 0.4082, -0.7071]
1100	$[\frac{1}{2}, \frac{1}{2}, -\frac{1}{2}, -\frac{1}{2}]$	[0.5774, 0.8165, 0]
1110	$[\frac{1}{4}, \frac{1}{4}, \frac{1}{4}, -\frac{3}{4}]$	[0.2887, 0.4082, 0.7071]
1000	$[\frac{3}{4}, -\frac{1}{4}, -\frac{1}{4}, -\frac{1}{4}]$	[0.8660, 0, 0]

The "**abc** coordinates" of the intersection of the ray from the center [0, 0, 0] of the rhombic dodecahedron through the projection $[\sqrt{3/4}w - \sqrt{1/12}(x+y+z), \sqrt{2/3}x - \sqrt{1/6}(y+z), \sqrt{1/2}(y-z)]$ of a chromatic point $[wxyz]$, and the boundary of the rhombic dodecahedron, gives a *hue* η. Since each chromatic triangle projects to a line segment, from the center of the rhombic dodecahedron to its boundary, η is the projection $[\mathbf{a}.\mathbf{h}, \mathbf{b}.\mathbf{h}, \mathbf{c}.\mathbf{h}]$ of $\mathbf{h}$. The distance $\sigma = \sqrt{w^2 + x^2 + y^2 + z^2 - 4\lambda^2}$ from the center of $\mathbf{D}$ to the point is a measure of chromatic saturation; also, the projection $[\lambda, \lambda, \lambda, \lambda]$, $\lambda := \frac{w+x+y+z}{4}$ on $\mathbf{A}$, gives a measure of luminance. In this way, an alternate colour space $\eta\lambda\sigma$ results.

2.4 A toroidal hue

The tint $\Theta \in \mathbf{S}^3$ of a colour $\mathbf{p}$ different from $\mathbf{g}$ is given by $\Theta = \mathbf{g} + \chi(\mathbf{p} - \mathbf{g})$ where $\chi = \frac{1}{2max\{|w'|,|x'|,|y'|,|z'|\}}$ where $w' = w - 0.5$, $x' = x - 0.5$, $y' = y - 0.5$ and $z' = z - 0.5$. The indexes i of the coordinates Θ_i of $\Theta = [\Theta_0, \Theta_1, \Theta_2, \Theta_3]$ of value 0 or 1 indicate the cube Θ is at; for example, if $\Theta_1 = 0$, then $\Theta \in \{x = 0\}$.

A coordinate system for the points in an $\mathbf{S}^3$ results by considering a Heegaard splitting of genus 1. It uses two angles and a "signed distance" $r \in [-1, 1]$, rather than the better-known, spherical coordinates of three angles. A Heegaard torus splits the 3-sphere into two open solid tori and their common boundary.

Out of the 24 square faces in $\mathbf{T}$, 16 faces can be chosen whose union $\mathbf{U}$ is a Heegaard torus for $\mathbf{T}$; this can be done in three ways since the 8 cubes in $\mathbf{T}$ can be grouped in $\frac{1}{2}\binom{4}{2} = 3$ ways, into two groups of four cubes each, so that each group is a solid torus. Here, we consider the solid tori $\mathbf{V}_{yz} := \{z = 0\} \cup \{y = 1\} \cup \{z = 1\} \cup \{y = 0\}$ and $\mathbf{V}_{wx} := \{w = 0\} \cup \{x = 1\} \cup \{w = 1\} \cup \{x = 0\}$. The boundaries of $\mathbf{V}_{wx}$ and $\mathbf{V}_{yz}$ are the torus $\mathbf{U}$; $\mathbf{U}$ can be seen as the union of four *square pipe segments* (stacks of squares) in two ways; each pipe segment (topological cylinder or annulus) is a stack of 1-squares that are meridians for the solid torus in question and longitudes for the other solid torus. For the solid torus $\mathbf{V}_{yz}$ we have the pipes of square meridians with vertices
$P_0 := \{(0, 0, s, 0), (1, 0, s, 0), (1, 1, s, 0), (0, 1, s, 0) : s \in [0, 1)\}$ (z=0),
$P_1 := \{(0, 0, 1, s), (1, 0, 1, s), (1, 1, 1, s), (0, 1, 1, s) : s \in [0, 1)\}$ (y=1),
$P_2 := \{(0, 0, 1 - s, 1), (1, 0, 1 - s, 1), (1, 1, 1 - s, 1), (0, 1, 1 - s, 1) : s \in [0, 1)\}$ (z=1) and
$P_3 := \{(0, 0, 0, 1 - s), (1, 0, 0, 1 - s), (1, 1, 0, 1 - s), (0, 1, 0, 1 - s) : s \in [0, 1)\}$ (y=0),
similarly, the boundary of the $\mathbf{V}_{wx}$ is given by the pipes of square meridians with vertices
$Q_0 := \{(0, t, 0, 0), (0, t, 1, 0), (0, t, 1, 1), (0, t, 0, 1) : t \in [0, 1)\}$ (w=0),

$Q_1 := \{(t,1,0,0),(t,1,1,0),(t,1,1,1),(t,1,0,1) : t \in [0,1)\}$ (x=1),
$Q_2 := \{(1,1-t,0,0),(1,1-t,1,0),(1,1-t,1,1),(1,1-t,0,1) : t \in [0,1)\}$ (w=1) and
$Q_3 := \{(1-t,0,0,0),(1-t,0,1,0),(1-t,0,1,1),(1-t,0,0,1) : t \in [0,1)\}$ (x=0).

As remarked, $\mathbf{U} = \cup P_i = \cup Q_i$. Each point of $\mathbf{T}$ is either in the open solid torus $\mathbf{V}_{wx}$, in the open solid torus $\mathbf{V}_{yz}$, or in their common boundary $\mathbf{U}$. The subindex n of the pipe segment together with the value of t or s, as in $n.t$, or $n.s$, give an angular measure that ranges from 0 to 4, mod-4.

For Θ in an open torus, there is a distance $r \neq 0$ from the boundary of the 2-square in the pipe the tint is at; the distance from the boundary is measured with the product metric; that is, for example, for the piece of solid torus bounded by pipe P_0, a tint point $[w,x,t,0]$ is at distance $0.5 - \max\{|w-0.5|, |x-0.5|\}$ from its boundary. There are two 1-squares in pipes, say P_n and Q_m, with corresponding parameters s and t such that one of them (a meridian) bounds the two-square the tint is in, and the other intersects the first square at a point $\mathbf{u} \in U$. Let $\mathbf{u} = (\phi_{wx}, \phi_{yz}) := (n.s, m.t)$ be the *toroidal hue* of $\mathbf{p}$; if Θ is on $\mathbf{U}$, let $r = 0$. Denote Θ as $(\phi_{wx}, \phi_{yz}, r)$; with the understanding that if $r = \pm 0.5$ (i.e. if Θ is precisely on the axis or core of a solid torus), exactly one of the angles ϕ or ψ is left undefined and only the longitude of the corresponding solid torus that contains Θ is specified. For example, the tint of $\mathbf{p} = [0.9,\ 0.2,\ 0.3,\ 0.4]$ is $[R, r, \phi_{wx}, \phi_{yz}] = [0.4000, 0.2500, 1.1250, 3.7500]$, at (product) distance 0.4 from the center of the hypercube, with Θ corresponding to pipes $w = 0$ and $y = 0$, with $s = 1/8$ (i.e. $x = 1/8$) and $t = 3/4$ (i.e. $z = 1/4$), inside $\mathbf{V}_{wx}$, at distance 0.25 from the boundary of the corresponding 2-square. Call r the *toroidal saturation*; its 3D analog would be the distance of a point in the boundary of the RGB cube to the chromatic hexagon.[8]

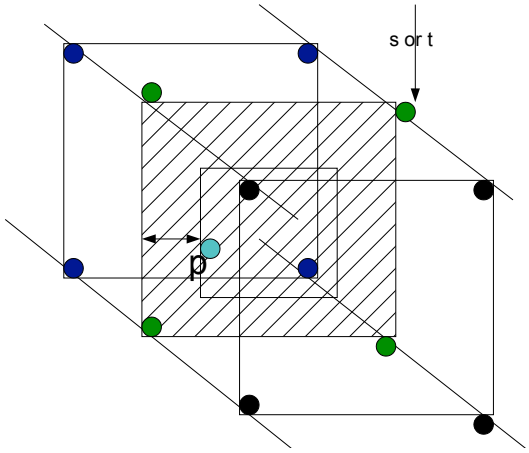

Figure 1. A pipe of $\mathbf{V}_{wx}$ or $\mathbf{V}_{yz}$. The squares in each pipe are indexed by the parameters s or t and provide the "decimal part" of the angles mod-4, $\phi_{wx} = n.s$ and $\phi_{yz} = m.t$.

2.5 Runge Ball

A 4D round space is obtained by deforming the hypercube into the standard 4-ball $\{(w',x',y',z') \in \mathbf{R}^4 : w^2+x^2+y^2+z^2 \leq 1\}$. This can be done in several ways; one is to deform the $\rho\mu$ triangle, into a semicircle and to spin it around $\mathbf{S}^2$, with hinge the μ basis of the triangle, where $\mathbf{S}^2$ is the chromatic dodecahedron deformed into a sphere. Another way is to spin the *midray* (that that originates at intermediate gray) around $\mathbf{S}^3$, with hinge the point of intermediate gray. In the first case we have a space with coordinates the luminance, the chromatic saturation and a 2D (the equatorial sphere derived from the chromatic dodecahedron) spherical hue; in the second case, we have a space with coordinates given by the generalized saturation r and a generalized 3D hue given by the $\mathbf{S}^3$ that is derived from the boundary of the hypercube.

Let $[w,x,y,z]$ be a point in the hypercube, shift the hypercube so that intermediate gray ends up at the origin of 4-space R^4 and rescale so that the maximum values of the coordinates is 1 and the minimum is -1. Let $[w',x',y',z'] = 2[w-0.5, x-0.5, y-0.5, z-0.5]$ be the coordinates of the resulting hypercube $[-1,1]^4$.

The *lightness* in this space is given by the angle with the achromatic axis: $\lambda = arcos\frac{w'+x'+y'+z'}{2\sqrt{w'^2+x'^2+y'^2+z'^2}} = arcos\frac{w+x+y+z-2}{2\sqrt{w^2+x^2+y^2+z^2+1-(w+x+y+z)}}$. Rather than using a chromatic saturation measure i.e. a distance measure to the achromatic line segment, we use a distance **g** obtaining a measure of colourfulness in the sense of "ungrayness". Let $\Lambda = max\{|w'|, |x'|, |y'|, |z'|\}$; if $\Lambda \neq 0$, the point on the boundary of the hypercube that is in the same direction is $\frac{1}{\Lambda}[w', x', y', z']$ (at least one of its coordinates has value of 1); let $d = \frac{1}{\Lambda}\sqrt{w'^2 + x'^2 + y'^2 + z'^2}$ and normalize by this length (with the result that the hypercube is deformed into a 4-ball), getting the point $\mathbf{s} = [s_0, s_1, s_2, s_3] := \frac{1}{d}[w', x', y', z']$ whose distance from the center of the ball is

$\kappa = \frac{\sqrt{w'^2+x'^2+y'^2+z'^2}}{\Lambda^{-1}\sqrt{w'^2+x'^2+y'^2+z'^2}} = \Lambda$. Thus

$\kappa = max\{2w-1, 2x-1, 2y-1, 2z-1\}$ is the *colourfulness* of the point $[w, x, y, z]$. $\chi = \frac{1}{2\Lambda}$.

3. RGBP: RGB+PANCHROMATIC

Another source of tetrachromatic images is computational photography. TrueSense imaging inc. markets a digital image sensor that, in addition to R, G, and B pixels, includes Panchromatic pixels (also called monochromatic, that are covered by the microlens but otherwise are not filtered) in a pattern as shown in Fig. 2. The proportions are 1/4 of green pixels, 1/8 of red pixels, 1/8 of blue pixels and 1/2 panchromatic pixels. Even though the photosensitive transducers respond well into the UV, the microlens blocks wavelengths below 350 nm. The sensor responds in the infrared but the response is negligible above 1050 nm.

Sorry for the delayed response, I was on vacation. Typically, we output the data in the pattern of the color filter array. Then the data is interpolated to get the three color channels (RGB). The pattern is

Figure 2. Pattern in the array of the sensor Truesense Imaging KAI-01150: P B P G; B P G P; P G P R; G P R P.

Since our objective is to explore the uses of tetrachromatic colour image processing, we do not interpolate the data in the image shown in but we convert each 4×4 pixel block into a tetrachromatic pixel, by averaging the pixels in each band in the block. Thus even though the original image is 1152×2044, the image we work with is 287×510 pixels. Also, the bands we use are $w = R$, $x = G$, $y = B$ and $z = P - (R + G + B)$, so, the z-primary is actually an approximation to a combination of NIR and UV wavelength bands. Something similar occurs in our visual system when the S and L channels are combined in a process opposed to the M channel (the other processes being L+M.vs.S, and (nonopposing) L+M+S.)

3.1 Tetrachromatic metamerism

The data provided by TrueSense of the quantum efficiency of each sensor type, at each 10 nm from 350 to 1100 nm, provides 76 data per band. We decided to work with these vectors and assume that the response to a light with equally sampled spectrum would be

$$\begin{bmatrix} w \\ x \\ y \\ z \end{bmatrix} = \begin{bmatrix} r_1 & ... & r_{76} \\ g_1 & ... & g_{76} \\ b_1 & ... & b_{76} \\ p_1 & ... & p_{76} \end{bmatrix} \begin{bmatrix} S_1 \\ . \\ .. \\ S_{76} \end{bmatrix}$$

The sampled responses of the sensor (courtesy of Keith Wetzel) provide a linear transformation $\mathbf{R}^{76} \rightarrow \mathbf{R}^4$. The kernel of this transformation is the orthogonal space to the subspace $M := span\{r, g, b, p\}$, and then any

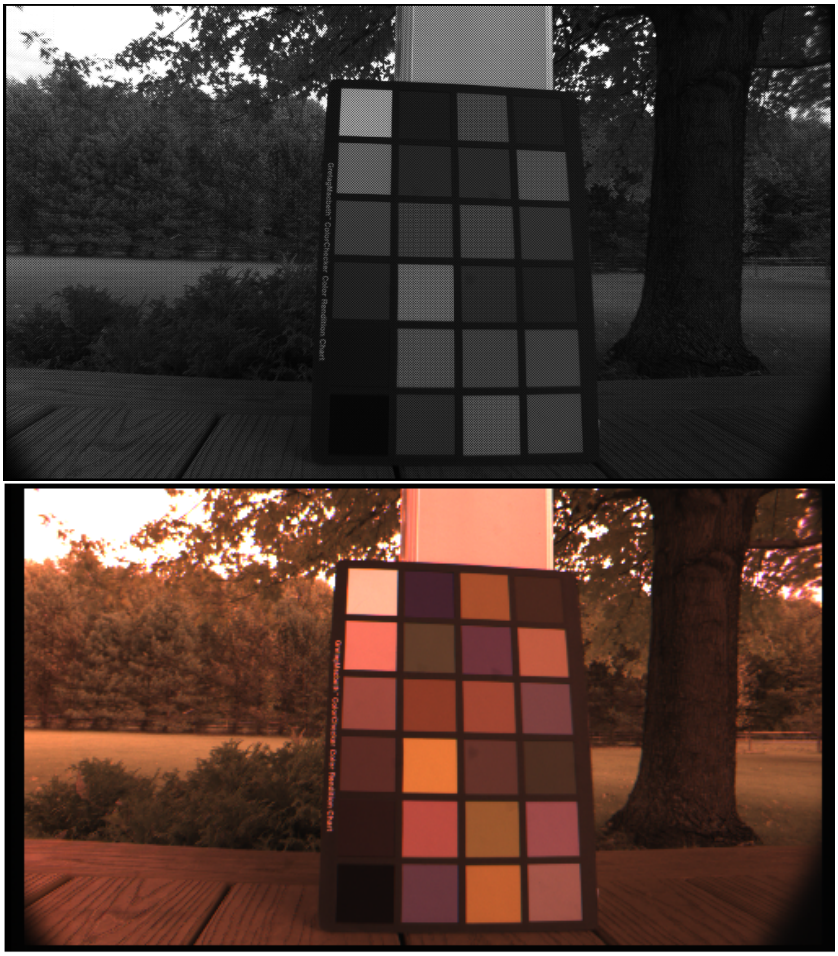

Figure 3. Outdoors, 16-bit, RGBP image of a Macbeth chart; courtesy of Amy Enge. Below, RGB visualization without corrections.

two spectra S^1 and S^2 such that $S^1 - S^2 \in M^\perp$ produce the same response $[wxyz]$. We provide a basis for $M^\perp$ which has dimension 72. We derive 3 triangular matrices of row vectors, in the first one M^1 we have a basis for the orthogonal complement of span(r), in the second one M^2 a basis for the orthogonal complement of spanr, g, then, in M^3 a basis for $(span\{r, g, b\})^\perp$ and finally, in M^4, a basis for $(span\{r, g, b, p\})^\perp$.

In $M^1_{76\times 75}$ the i^{th} row (the diagonal is a diagonal of 1's) looks like $[0, ..., 0, 1, -r_i/r_{i+1}, 0, ..., 0]$. By making sure a linear combination of each two consecutive rows in $M^1_{76\times 75}$ is orthogonal to g, you get for example $M^2_{76\times 74}$ with i^{th} row given by $[0, ..., 0, 1, m_{i,i+1} + \beta m_{i+1,i+1}, \beta m_{i+1,1+2}, 0, ..., 0]$ (the diagonal of $M^2_{76\times 74}$ is a diagonal of 1's), where the m's are the components of $M^1_{76\times 75}$ and $\beta = -\frac{g_i + m_{i,i+1} g_{i+1}}{m_{i+1,i+1} g_{i+1} + m_{i+1,i+2} g_{i+2}}$.

Likewise, by making sure a linear combination of each two consecutive rows in $M^2_{76\times 74}$ is orthogonal to b, one obtains $M^3_{76\times 73}$ whose i^{th} row looks like $[0, ..., 0, 1, m_{i,i+1} + \beta m_{i+1,i+1}, m_{i,i+2} + \beta m_{i+1,i+2}, \beta m_{i+1,1+3}, 0, ..., 0]$ (the diagonal is a diagonal of 1's), where the m's are the components of $M^2_{76\times 74}$ and
$\beta = -\frac{b_i + b_{i+1} m_{i,i+1} + b_{i+2} m_{i,i+2}}{b_{i+1} m_{i+1,i+1} + b_{i+2} m_{i+1,i+2} + b_{i+3} m_{i+1,i+3}}$.

Finally, a linear combination of each two consecutive rows in $M^3_{76\times 73}$ that is orthogonal to p, one obtains $M^4_{76\times 72}$ with i^{th} row $[0, ..., 0, 1, m_{i,i+1} + \beta m_{i+1,i+1}, m_{i,i+2} + \beta m_{i+1,i+2}, m_{i,i+3} + \beta m_{i+1,i+3}, \beta m_{i+1,1+4}, 0, ..., 0]$, where the m's are the components of $M^3_{76\times 73}$ and
$\beta = -\frac{b_i + b_{i+1} m_{i,i+1} + b_{i+2} m_{i,i+2} + b_{i+3} m_{i,i+3}}{b_{i+1} m_{i+1,i+1} + b_{i+2} m_{i+1,i+2} + b_{i+3} m_{i+1,i+3} + b_{i+4} m_{i+1,i+4}}$.
The basis elements in are shown in Fig. 5. The rows in $M^1_{76\times 75}$ have support of length 2, those in $M^2_{76\times 74}$ have

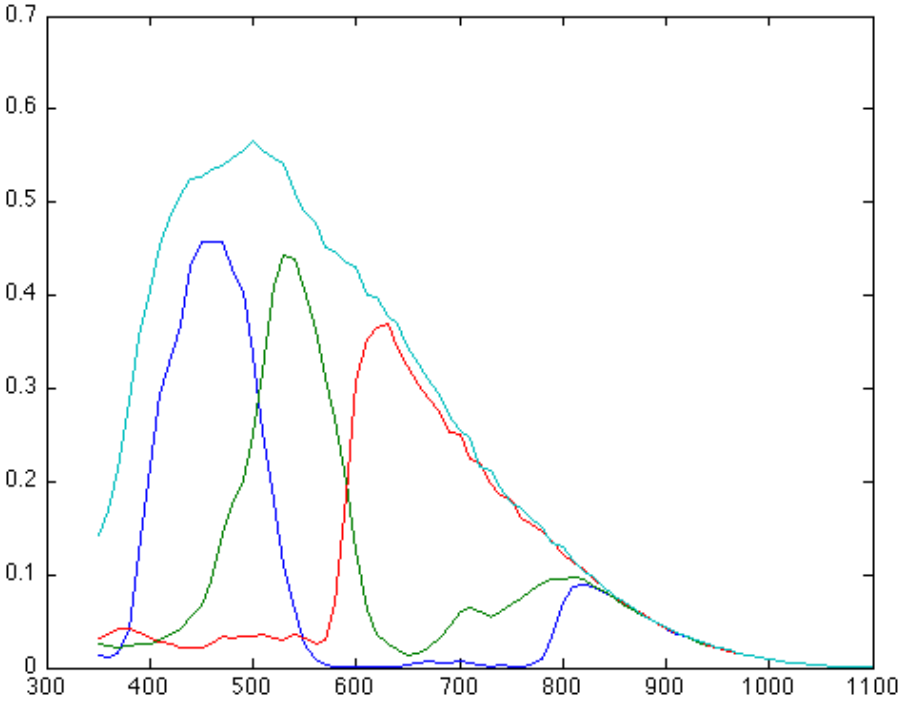

Figure 4. Quantum efficiencies corresponding to Truesense sensors.

support of length 3, those in $M^3_{76\times 73}$ have support of length 4 and those in the basis $M^4_{76\times 72}$ of $(span\{r,g,b,p\})^\perp$ have support of length 5. See Fig. 5.

4. PROCESSING

The application of a law to each pixel of a tetrachromatic image produces a new tetrachromatic image that can then be visualized or fed to a computer vision algorithm. By appropriately modifying the hue, it is possible to visualize tetrachromatic images in such a way that certain aspects are made conspicuous, or more aesthetic.

Simple modification types of tetrachromatic hue are given by rotations of the 2-sphere, of the 3-sphere, or of the Heegaard torus.In the Runge 4-ball, with boundary $\mathbf{S}^3$, a point can be expressed as (d,Θ). A point $\Theta\in\mathbf{S}^3$ can be expressed for example as a point in $\mathbf{R}^4$ of unitary norm, equivalently as a quaternion or, in "spherical coordinates," with three angles θ,ϕ,ψ. We propose yet another coordinate system based on a Heegaard torus for $\mathbf{S}^3$.

The space of rigid motions of $\mathbf{S}^3$ (the rotations of $\mathbf{R}^4$) has the group structure SO(4); it is the topoloical space $\mathbf{S}^3\times\mathbf{RP}^3$ for which $\mathbf{S}^3\times\mathbf{S}^3$ is a double cover.[§] To modify the generalized hue in a basic way, a rigid motion of $\mathbf{S}^3$ is implemented; such motions can be coded as a pair $(\theta_1,\theta_2)\in\mathbf{S}^3\times\mathbf{S}^3$ and are implemented by pre and post multiplying a unit quaternion (s$\in\mathbf{S}^3$) times unit quaternions p and q, as in psq. The space $\mathbf{H}$ of the quaternions can be seen as $(\mathbf{R}^4,+,\times)$ or as $(\mathbf{C}^2,+,\times)$. For $\mathbf{C}^2$, the analogous case of an orthogonal transformation is that of a unitary transformation that rather than preserving the structrure of the inner product in $\mathbf{R}^2$, it preserves the standard hermitian form $(z_1,z_2).(w_1,w_2)=z_1\bar{w}_1+z_2\bar{w}_2$; a point of $\mathbf{S}^3$ is also denoted as a pair $(z_1,z_2)\subset\mathbf{C}^2$, with $z_1\bar{z_1}+z_2\bar{z_2}=1$ The rigid motions of $\mathbf{S}^2$ are implemented by pre and post multyplying a pure quaternion s times a unit quaternion q and its conjugate, as in qsq^*.

The hue can thus be independently processed of the luminance (and saturation), by automorphisms (could be PL in particular) either of the 3-sphere, a hue sphere or of a hue torus. There are 8 (intersecting) dodecahedra (PL topological spheres) in the complex $\partial\mathbf{I}^4$ and also three (intersecting) PL Heegaard tori, so it is possible to

[§]The set of rotations of the plane is the group SO(2) which has the topology of $\mathbf{S}^1$ while the set of rigid motions of $\mathbf{S}^2$ (of rotations of $\mathbf{R}^3$) is the group SO(3) which has the topology of $\mathbf{RP}^3$.

modify an image in multiple ways. As the hue surfaces are rotated or otherwise *automorphed*, the colours of a tetrachromatic image change in interesting ways. The automorphisms respect the continuity; the rotations are isometries and respect the antipodicity or complementary colours as well.

For toroidal hue, for PL rotations, the 1D squares with sides parallel to the axes w and x are meridians of the yz solid torus and longitudes of the wx solid torus; the 1D squares with sides parallel to the axes y and z are meridians of the wx solid torus and longitudes of the yz solid torus. Similarly for the other cases. Shifts around such squares implement modifications of hue. The automorphisms of the torus can be characterized with a process of cut and twist, as in;[9] then, an automorphism of each solid torus is obtained by extending the automorphism of its boundary in such a way that it is the identity on its core and the amount of twisting gradually increases towards its boundary.

The linear (i.e. noncircular, nonspherical) coordinates such as colourfulness, chromatic saturation and luminance, are transformed here via exponential-law maps x^γ, $\gamma \in (0, \infty]$.

As examples, consider the image in Fig. 6; it has been processed in Runge space in Fig. 7 and in toroidal space in Fig. 8. Also, the image in Fig. 3, has been processed in toroidal space in Fig. 9; in this case, the band w is the difference between the averages of R, G and B, and the average of P.

5. CONCLUSIONS

Tetrachromatic colour spaces find applications in the visualization of 4-spectral images and the modeling of tetrachromatic vision systems. Its use in satellite imaginery[10] is likely since it provides alternate ways to the mere feeding of the visualizing RGB channels with permutations of the image wxyz channels.

As a technique for computational photography, the exploitation of IR and UV bands is likely to be of use in different ways, for example, increasing or decreasing detail, and also as hints for the modification of RGB colour. There may be a problem of chromatic aberration here, as the paths of different wavelengths, i.e. those of UV and NIR, may focus at different planes. Further work remains to be done in the exploitation of automorphisms of spheres and tori, different from isometries. Depending on the application different types of tetrachromatic colour processing will be needed.

Existent linear techniques for smoothing and contrast enhancing such as the moving average, the moving median and unsharp masking, can be extended not only to the circular case[11] but also to spherical cases.

The visualization of tetrachromatic images can me tackled as well with movie sequences where a few frames that are fed to the RGB channels of a projector and that result from 3 of the four bands of processed versions of the tetrachromatic image.

APPENDIX A: Matlab code

Kernel of [p;r;g;b]:

```
    function[AL4] = TrueSense(AC)
ALREV=[B,G,R,P];
figure; plot(L,ALREV);
AL1= zeros(76,75);
for ii=1:75
AL1(ii,ii)= 1;
AL1(ii,ii+1)= -R(ii)/R(ii+1);
end
figure; plot(L,AL1)
AL2= zeros(76,74);
for ii=1:74
AL2(ii,ii)= 1;
BETA= -(G(ii) + G(ii+1)*AL1(ii,ii+1)/AL1(ii,ii))/(AL1(ii+1,ii+1)*G(ii+1) + AL1(ii+1,ii+2)*G(ii+2));
AL2(ii,ii+1)= AL1(ii,ii+1)/AL1(ii,ii) + BETA*AL1(ii+1,ii+1);
AL2(ii,ii+2)= BETA*AL1(ii+1,ii+2);
```

```
end
figure; plot(L,AL2)
AL3= zeros(76,73);
for ii=1:73
AL3(ii,ii)= 1;
BETA= -(B(ii) + B(ii+1)*AL2(ii,ii+1)/AL2(ii,ii) + B(ii+2)*AL2(ii,ii+2)/...
AL2(ii,ii))/(B(ii+1)*AL2(ii+1,ii+1) + B(ii+2)*AL2(ii+1,ii+2) + B(ii+3)*AL2(ii+1,ii+3));
AL3(ii,ii+1)= AL2(ii,ii+1)/AL2(ii,ii) + BETA*AL2(ii+1,ii+1);
AL3(ii,ii+2)= AL2(ii,ii+2)/AL2(ii,ii) + BETA*AL2(ii+1,ii+2);
AL3(ii,ii+3)= BETA*AL2(ii+1,ii+3);
end
figure; plot(L,AL3)
AL4= zeros(76,72);
for ii=1:72
AL4(ii,ii)= 1;
BETA= -(B(ii) + B(ii+1)*AL3(ii,ii+1)/AL2(ii,ii) + B(ii+2)*AL3(ii,ii+2)/AL2(ii,ii)) + B(ii+3)*AL3(ii,ii+3)/AL3(ii,ii)/...
(B(ii+1)*AL3(ii+1,ii+1) + B(ii+2)*AL3(ii+1,ii+2) + B(ii+3)*AL3(ii+1,ii+3)) + B(ii+4)*AL3(ii+1,ii+4);
AL4(ii,ii+1)= AL3(ii,ii+1)/AL3(ii,ii) + BETA*AL3(ii+1,ii+1);
AL4(ii,ii+2)= AL3(ii,ii+2)/AL3(ii,ii) + BETA*AL3(ii+1,ii+2);
AL4(ii,ii+3)= AL3(ii,ii+3)/AL3(ii,ii) + BETA*AL3(ii+1,ii+3);
AL4(ii,ii+4)= BETA*AL3(ii+1,ii+4);
end
```

APPENDIX B: Spinning

Let $I = [0, 1]$ and let $A \subset I^n$; also, let $H \subset A$. Topologically, the *spin of A with $\mathbf{S}^m$ with hinge H* is the quotient space $A \times \mathbf{S}^m$ modulo the equivalence relation with corresponding equivalence classes of the form $E_h = \{(h, s) | s \in \mathbf{S}^m\}$, for each $h \in H$.

REFERENCES

[1] Restrepo, A., "Tetrachromatic colour space," *SPIE Electronic Imaging, San Francisco* (2012).

[2] Restrepo, A., "Tetrachromatic colour spaces," *Visapp Rome* (2012).

[3] Hirakawa, K. and Parks, T., "Aditive homogeneity/directed demosaicing algorithm," *IEEE trans. on Image Processing* (2005).

[4] Enge, A., "Accurate color with increased sensitivity using ir," *SPIE, Electronic Imaging, San Francisco* (2012).

[5] Susstrunk, S., "Improving the visible with the invisible: Incorporating near-infrared cues in computational photography and computer vision," *Visapp, Rome* (2012).

[6] www.truesenseimaging.com, "Image sensor color correction. rev. 1.0 ps-0048," (2012).

[7] Hatcher, A., [*Algebraic topology*], Cambridge University Press, Cambridge (2002).

[8] Restrepo, A., "Colour processing in runge space," *SPIE Electronic Imaging, San Francisco* (2011).

[9] Lickorish, W., "A representation of orientable combinatorial 3-manifolds," *The Annals of Math. 2nd Ser.* **76**, 531–540 (1962).

[10] Landsat, "http://zulu.ssc.nasa.gov/mrsid/tutorial/ landsat%20tutorial-v1.html," (2012).

[11] A. Restrepo, C. R. and Vejarano, C., "Circular processing of the hue variable," *VISAPP 2007*, 69–76 (2007).

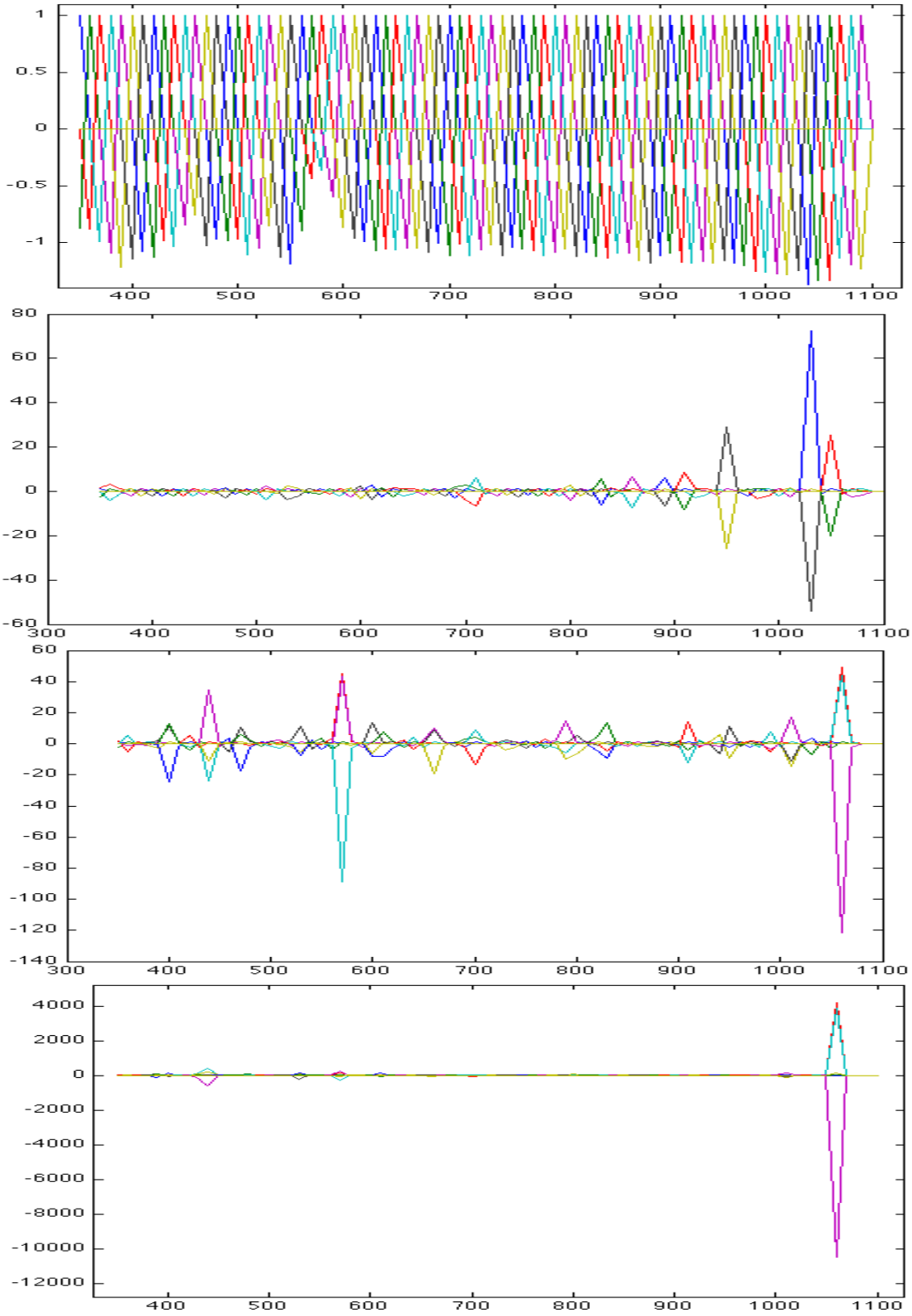

Figure 5. Kernel of [r; g; b; p] : $\mathbf{R}^{76} \rightarrow \mathbf{R}^{4}$.

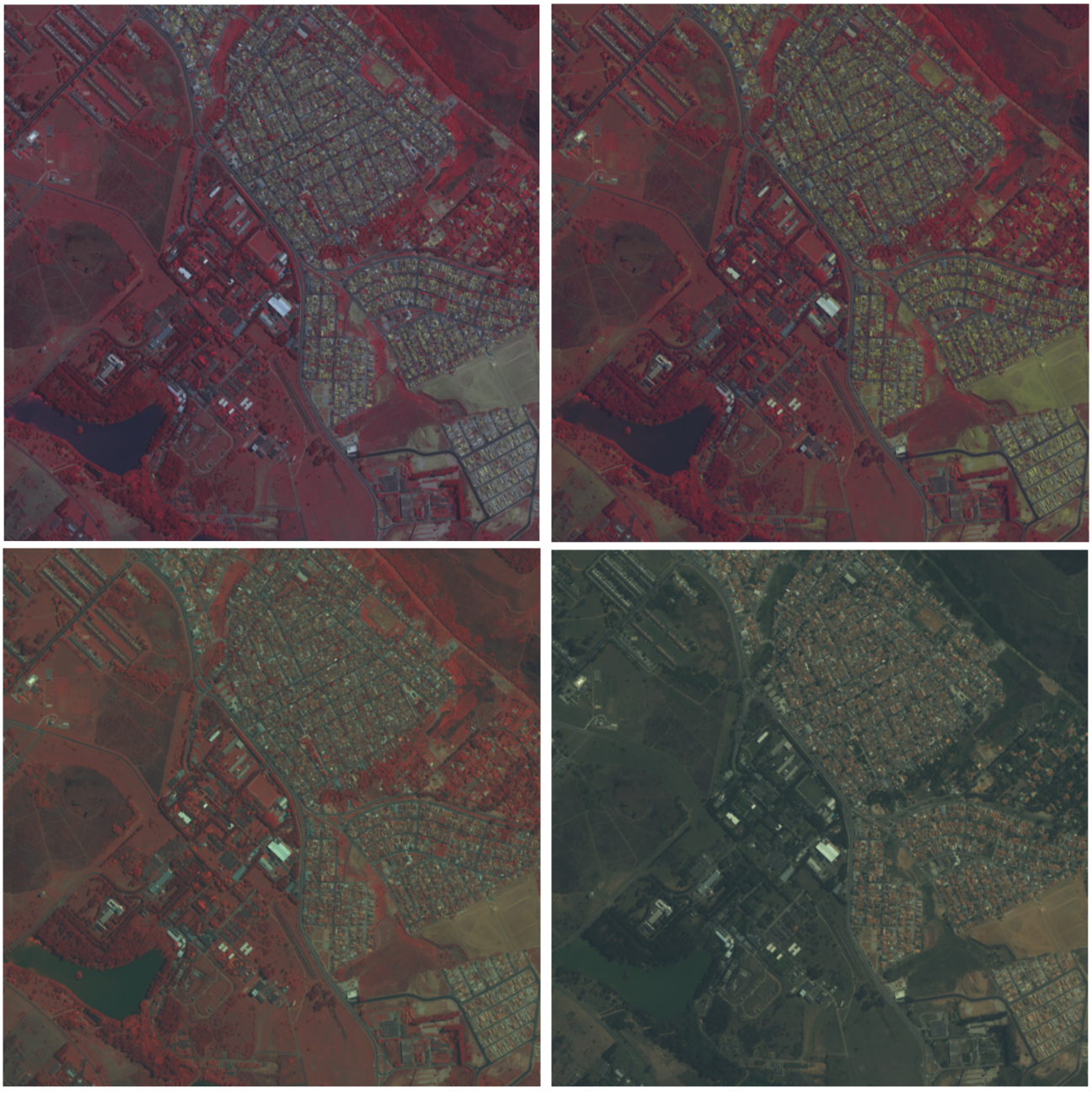

Figure 6. Original tetrachromatic image. Tetrachromatic bands NIR,R,G; NIR,R,B; NIR,G,B and RGB are fed to visualizing channels R, G, B.

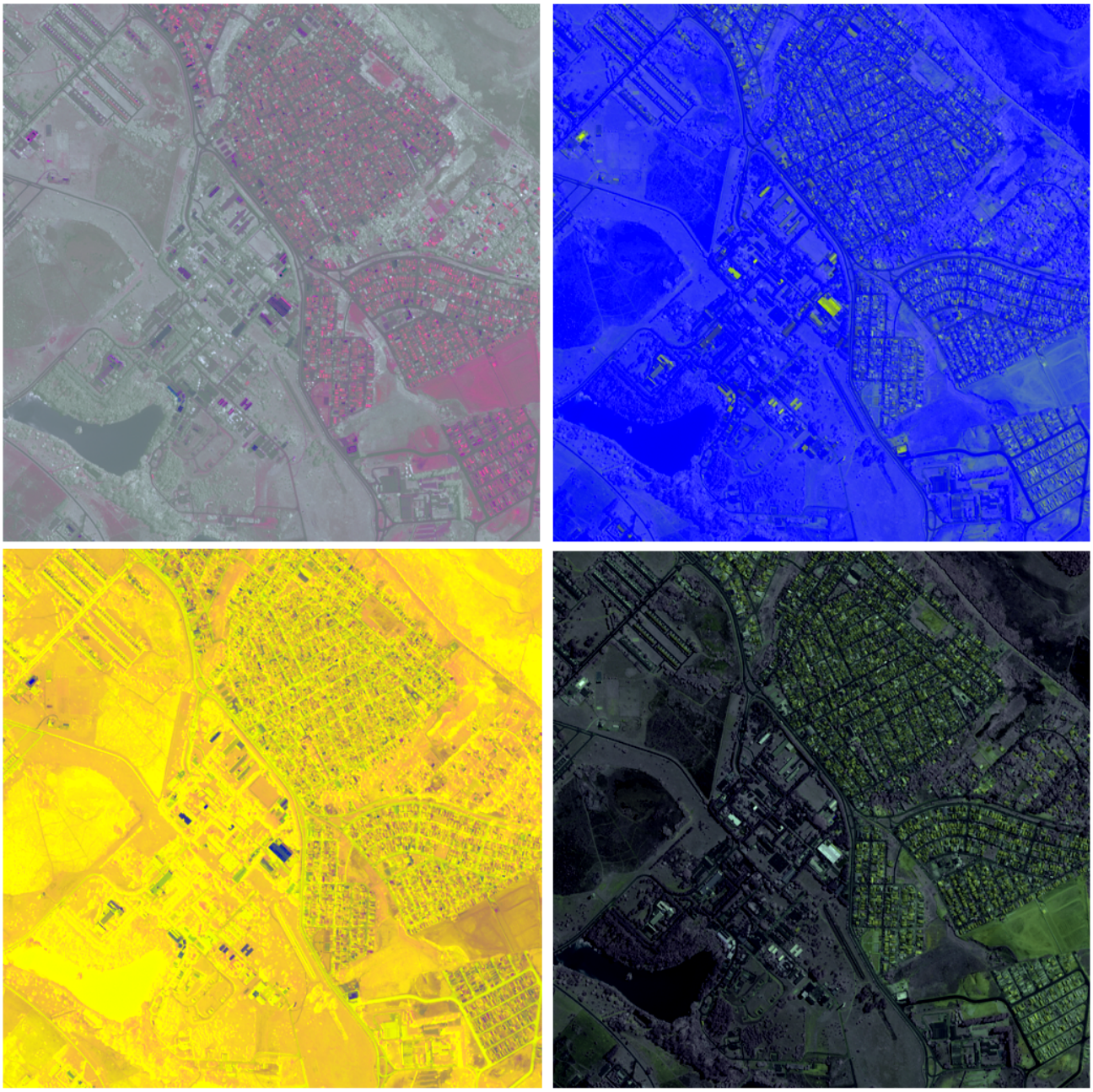

Figure 7. (Θ, d) processing: $(s, d) \mapsto (psq, d^{\gamma})$. p=[1/2, 1/2, -1/2, -1/2], q=[-1/2, -1/2, 1/2, 1/2], $\gamma = 0.6$; bands 1 (in R), 3 (in G), 4 (in B). p=[1/2, 1/2, 1/2, -1/2], q=[1/2, -1/2, 1/2, 1/2], $\gamma = 1.0$; bands 1, 2 and 3. p=[1/2, 1/2, 1/2, -1/2], q=[-1/2, 1/2, 1/2, 1/2], $\gamma = 1.0$; bands 2, 3 and 4. p=[1/2, 1/2, 1/2, -1/2], q=[1/2, -1/2, 1/2, 1/2], $\gamma = 1.0$; bands 1, 2 and 4.

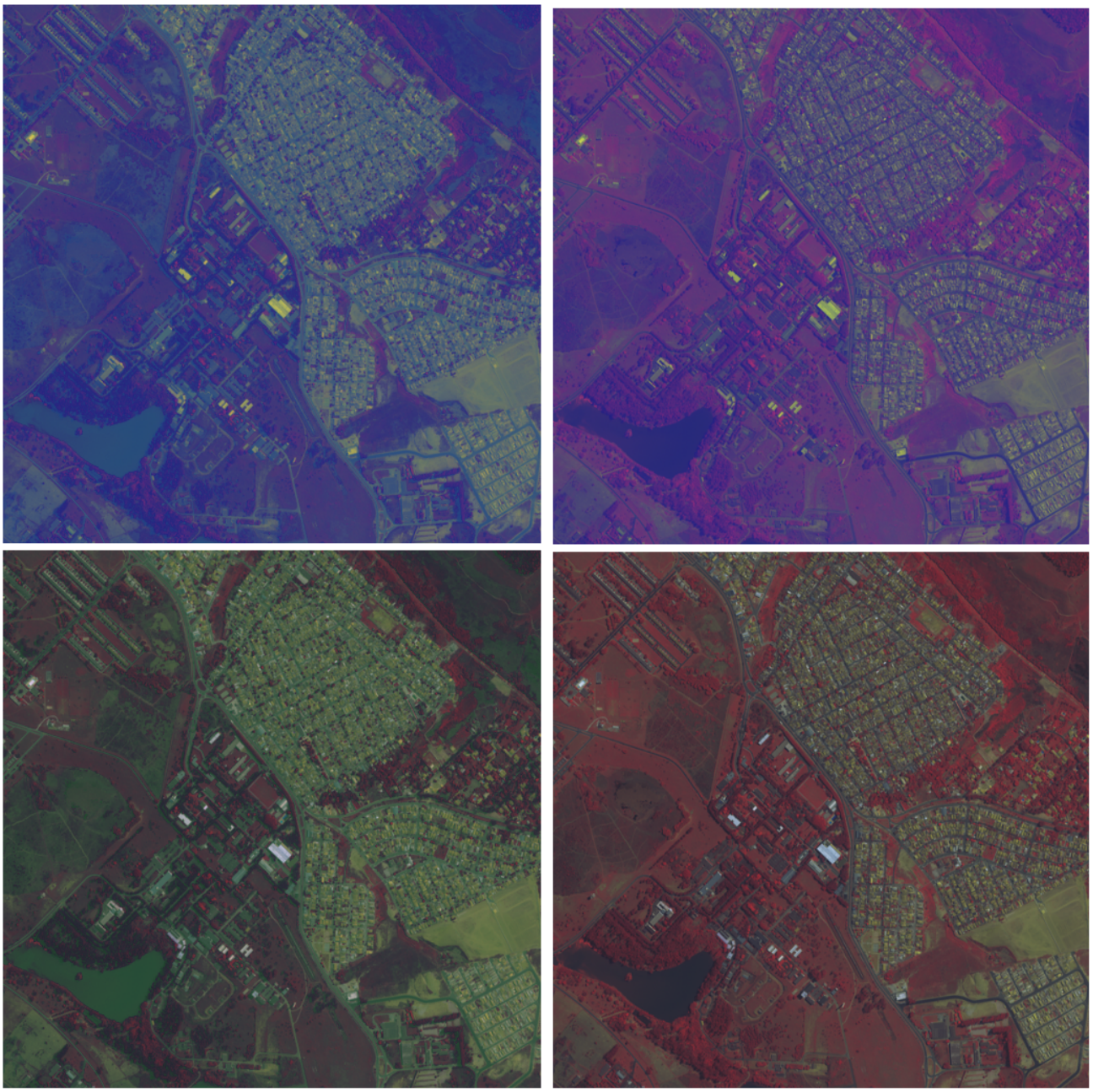

Figure 8. Torus processing. $(\phi_{wx}, \phi_y z) \mapsto (\phi_{wx} + 0.2, \phi_y z + 0.5)$, bands 124; $(\phi_{wx}, \phi_y z) \mapsto (\phi_{wx}, \phi_y z + 0.5)$, bands 124; $(\phi_{wx}, \phi_y z) \mapsto (\phi_{wx} + 0.2, \phi_y z + 0.2)$, bands 124; $(\phi_{wx}, \phi_y z) \mapsto (\phi_{wx}, \phi_y z + 0.5)$, bands 123.

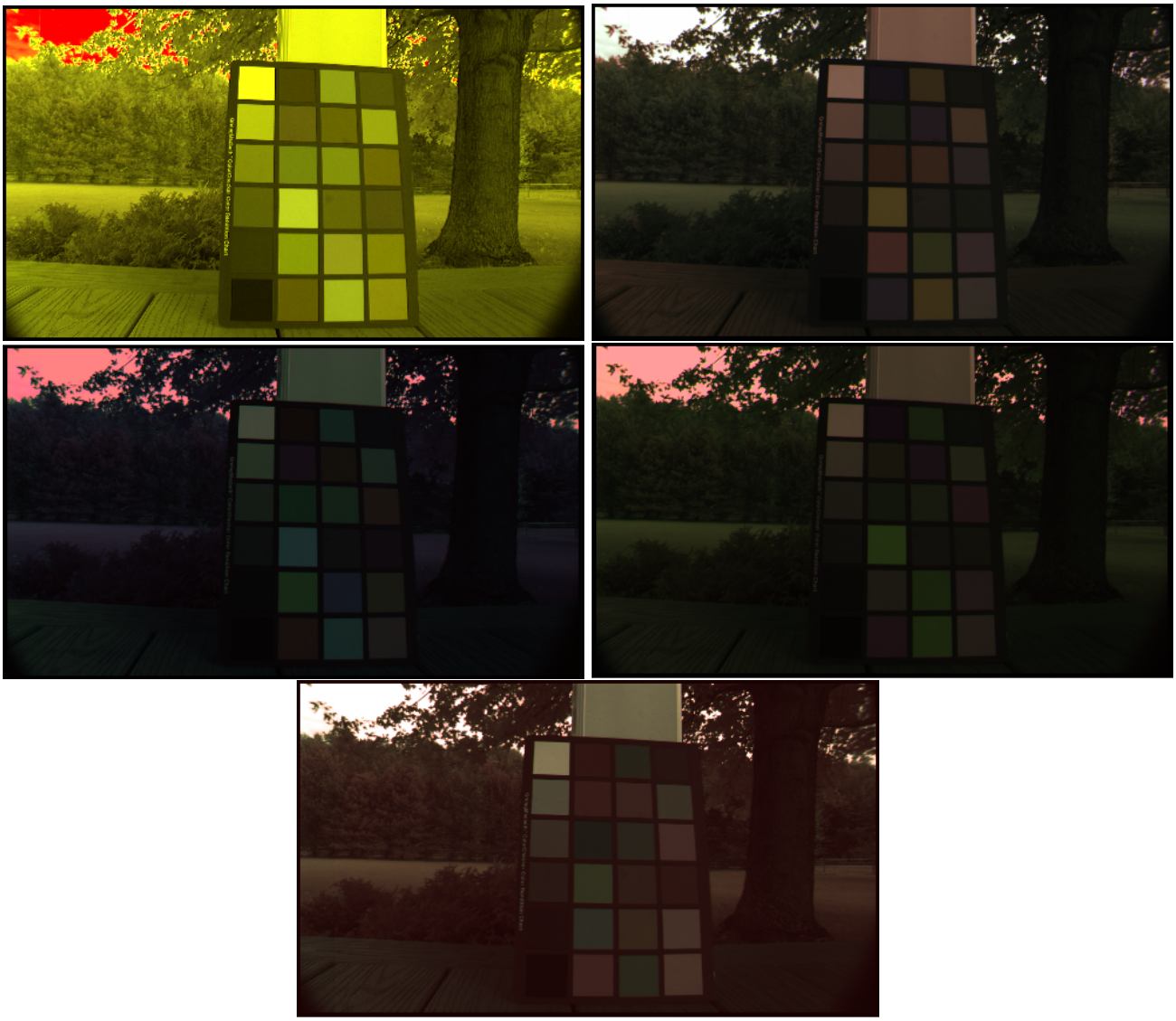

Figure 9. Corrections $R^{\gamma 1}$, $r^{\gamma 2}$, $\phi_{wx} + \Delta_{wx}$, $\phi_{yz} + \Delta_{yz}$; in (R, Θ) coordinate space system, where $\Theta = (r, \phi_{wx}, \phi_{yz})$. From top left, $\gamma 1 = 1$, $\gamma 2 = 0.7$, $\Delta_{wx} = 0$, $\Delta_{yz} = 0$, visualized with $RGB \leftarrow wxy$; $\gamma 1 = 1$, $\gamma 2 = 1.3$, $\Delta_{wx} = 0$, $\Delta_{yz} = 0$, visualized with $RGB \leftarrow wyz$; $\gamma 0.5 = 1$, $\gamma 2 = 1.5$, $\Delta_{wx} = 0$, $\Delta_{yz} = 0$, visualized with $RGB \leftarrow wxy$; $\gamma 1 = 0.6$, $\gamma 2 = 1.4$, $\Delta_{wx} = 0$, $\Delta_{yz} = 0$, visualized with $RGB \leftarrow wyz$ and $\gamma 1 = 1.1$, $\gamma 2 = 1.4$, $\Delta_{wx} = 0.005$, $\Delta_{yz} = -0.1$, visualized with $RGB \leftarrow wxy$. The w component is given by the difference $(R_{average} + G_{average} + B_{average}) - PAN_{average}$, and the x, y, z components are the signals $R_{average}$, $G_{average}$ and $B_{average}$, respectively.